SOLAR DRIVEN HYDROGEN FROM PHOTOCATALYTIC WATER SPLITTING

Khadija tul Kubra [1], M. S. Rafique [1], K. Siraj [1], R. Sharif [1], A. Ghaffar [2]
[1] Department of Physics, University of Engineering & Technology, Lahore 54890, Pakistan
[2]Department of Chemistry, university of Engineering & Technology, Lahore 54890, Pakistan
Corresponding author: Khadija.khan14@yahoo.com

ABSTRACT: *The water splitting has been performed directly in the sunlight to produce hydrogen using an artificial leaf. The artificial leaf comprises of a mono crystalline silicon based uncovered solar cell interfaced by oxygen-evolving catalyst (OEC) and hydrogen-evolving catalyst (HEC). Solar cell was used to harness light, Co-P_i served as OEC and NiMoZn-alloy as HEC. The focus was to explore the dependence of efficiency of the leaf on the area of electrodes. The catalysts were prepared by potentiostatic as well as by direct current electrodeposition on small and bigger surface area of the electrodes respectively. The various properties of the catalysts were analyzed by using cyclic voltammetry, Optical microscope, Scanning Electron Microscope (SEM) and Energy-Dispersive X-rays (EDX). The bigger area artificial leaf with OEC and HEC (with additives) was found to be most efficient to perform the hydrogen and oxygen evolution reaction when put in water in the presence of sunlight.*

Keywords: Artificial photosynthesis; Oxygen-evolving catalyst; Hydrogen-evolving catalyst; Solar cell; Photocatalytic water splitting.

1. INTRODUCTION

The global energy demand has increased manifold which has motivated the searchers for renewable fuel options instead of just relying on the fossil fuel reserves [1]. Solar energy is an attractive renewable energy source having much more potential than the fossil fuels. During the last few decades, the scientific community has been working to accomplish the possibility of producing solar fuels [2]. Nature has developed a way for utilizing the solar energy called Photosynthesis. The photochemical reaction in photosynthesis is a redox reaction which is initiated by the absorption of light through photosystems. The photosystems are the protein-complexes that participate in light absorption, energy conversion and electron transfer reactions. These protein-complexes are photosystem II (PSII) and photosystem I (PSI) with light harvesting complex II and I respectively. Photosystem II uses light energy to oxidize two molecules of water into one molecule of oxygen, four electrons and four protons. The four electrons and four protons removed from the water molecules are transferred to Photosystem I by an electron transport chain to reduce $NADP^+$ (Nicotinamide Adenine Dinucleotide Phosphate) into NADPH (reduced form of $NADP^+$). Later in the process, NADPH is used to form glucose, which is a main basis for energy in most organisms. The basic equation of oxygenic photosynthesis can be written as [3,4]:

$$6CO_2 + 6H_2O \xrightarrow[\text{chlorophyl II}]{\text{light energy}} C_6H_{12}O_6 + 6O_2 \quad (1)$$

It is vital to use solar energy for practical uses. To do this, photosynthesis offers an eminent approach for designing an artificial photocatalytic system for clean and sustainable fuel generation [5]. Artificial photosynthesis can replicate the natural photosynthesis by developing a device to produce hydrogen solar fuel. To design a wireless photocatalytic water splitting device, light is absorbed by a silicon solar cell. A general approach for mimicking photosynthesis using silicon solar cell is to interface
OEC and HEC on semiconductor photoanode (n-side) and photocathode (p-side), respectively. [6,7,8].

When a photon with energy greater than the band gap of a semiconductor interacts with an electron then it is excited from the valence band into conduction band in order to create an electron-hole pair. A photocatalytic hydrogen production involves both the oxidation of electron with hole and proton reduction with electron. This is the catalytic activity of the photocatalytic electrodes to trap the holes and electrons for performing the oxidation and reduction reaction under the voltage generated by sun illumination. The photocatalytic water splitting reactions are shown in Eqs. (2) – (4) [9,10]:

$$2H_2O \rightarrow O_2 + 4H^+ + 4e \quad \textbf{(Water oxidation half reaction)} \quad (2)$$

$$4H^+ + 4e^- \rightarrow 2H_2 \quad \textbf{(Proton reduction half reaction)} \quad (3)$$

$$2H_2O \rightarrow 2H_2 + O_2 \quad \textbf{(Overall water splitting reaction)} \quad (4)$$

Many researchers are working for making solar fuel by mimicking natural photosynthesis. The objective of this present work is to produce hydrogen solar fuel more efficiently from sunlight. The main challenge lies in the efficiency of solar fuel generation using bigger area artificial leaf. The three artificial leaves were fabricated and the H_2-generation experiment was optimized by performing on small area artificial leaf of dimension (1.5×1.5 cm^2), bigger area artificial leaf (15×15 cm^2) with OEC and HEC (under no additives) and bigger area artificial leaf (15×15 cm^2) with OEC and HEC (under additives).

2. EXPERIMNTAL DETAILS

2.1. Materials

The chemicals used in the present work are Cobalt (II) Sulfate monohydrate (CoSO4.H2O), potassium hydrogen Phosphate (K2HPO4), Nickel (II) Sulfate Heptahydrate (NiSO4.7H2O), Sodium molybdate (Na2MoO4), Anhydrous Zinc Chloride (ZnCl2), Sodium pyrophosphate decahydrate (Na4P2O7.10H2O), Sodium bicarbonate (NaHCO3), Hydrazine monohydrate (N2H4O), Nitric acid (HNO3) and Sodium hydroxide (NaOH).

2.2. Function of OEC and HEC

The cobalt salt in phosphate-buffered solution is used to produce Co-P_i (OEC) to increase the water oxidation efficiencies. The addition of phosphate is done to increase the conductivity and assists to transfer proton-electron couple for O_2 evolution [3]. The mixtures of metals increase the catalytic activity for hydrogen evolution [11]. In NiMoZn-alloy (HEC), Ni-metal shows significant chemical activity and it can increase the active surface area on which reaction can occur. Molybdenum-metal is a stable catalyst and it can leach from the alloy to furnish high surface area material. Zinc-metal plays an important role in chemical activity. Sodium pyrophosphate decahydrate, Sodium bicarbonate and Hydrazine monohydrate are used as additives. Nitric acid and Sodium hydroxide are used for attaining the required pH value.

2.3. Preparation of catalysts and characterization

An artificial leaf was developed as a light-harvesting device based on artificial photosynthesis. It comprised of pn-junction Si solar cell interfaced by Co-P_i based catalyst as OEC and NiMoZn-alloy catalyst as HEC. The both sides of the semiconductor surfaces were protected by conducting substrates. The n-side concealed by Indium Tin Oxide (ITO) coated glass substrate on which OEC was electrodeposited and the p-side was interlinked by stainless steel substrate on which HEC was electrodeposited [12]. The electrical contact was made between solar cell and catalyst coated substrates through conductive adhesive copper tape. The self-fabricated artificial leaf is shown in Fig. 1.

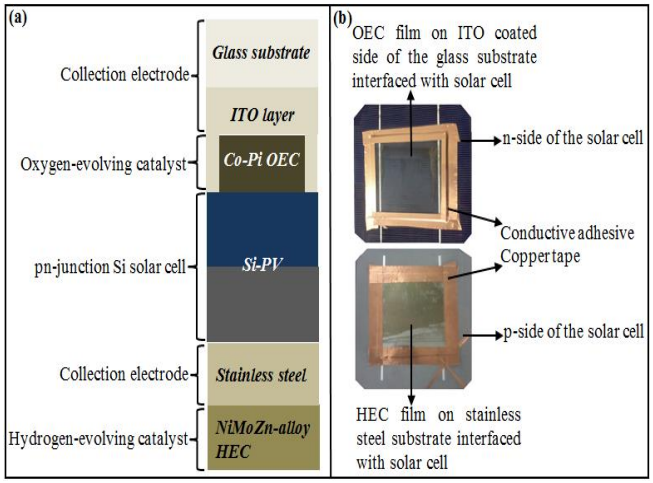

Fig. 1- The self-fabricated artificial leaf (a) Schematic of artificial leaf
(b) Photographs of both sides of artificial leaf.

In this artificial leaf, solar photons are absorbed by the silicon solar cell. The role of OEC and HEC is to suppress the charge recombination. The electrons and holes are shifted to the surface of the semiconductor where the catalysts coated substrates hold these charges [9]. The ITO coated glass substrate collects photo-produced holes which are transferred to the Co-P_i (OEC) film, where they participate in water oxidation reaction to produce O_2 when artificial leaf is put into the water. The electrons and protons are produced as by-products of the OEC reaction and thus protons are transferred to the stainless steel substrate having photo-produced electrons, where they are reduced to form H_2 when they reach to NiMoZn-alloy (HEC) film [7]. Hence, the photocatalytic H_2 production involves the redox reaction. The overall reaction rate is equivalent to both oxidation and reduction reactions.

The thin films of the Co-P_i (OEC) and NiMoZn-alloy (HEC) were prepared by electrodeposition under controlled parameters in an electrochemical cell. Catalysts films were prepared on small as well as on bigger surface area electrodes through potentiostatic electrodeposition (pulse current) and direct current (D.C.) electrodeposition respectively. The electric parameters (voltage, current) and deposition time were optimized to achieve the better deposition [13,14].

The potentiostatic electrodeposition of the Co-P_i (OEC) was performed by using a conventional three electrode system in an aqueous solution. Electrodeposition assembly comprised of ITO coated glass acting as working electrode and graphite as counter electrode of equal size (1×1 cm^2) and Saturated Calomel Electrode (SCE) as a reference electrode [15]. The ITO coated glass substrate was cleaned with acetone in the ultrasonic bath and then dried in air. The electrolyte of pH 7.0 was prepared by dissolving 0.5 mM/0.1L $CoSO_4.H_2O$ and 0.1 M/0.1L K_2HPO_4. The prepared electrolyte was then deposited on ITO coated glass substrate at room temperature (25 °C) for 30 minutes, which was used as a cathode and kept at an applied voltage of -1.23 V relative to the reference electrode [16,17].

The potentiostatic electrodeposition of the NiMoZn-alloy (HEC) was also performed by using a conventional three electrode system in an aqueous solution. Electrodeposition assembly comprised stainless steel substrate acting as working electrode and graphite as counter electrode of equal size (1×1 cm^2) and SCE as a reference electrode [15]. The stainless steel substrate was polished with successively finer grades of emery paper, cleaned in the ultrasonic bath and then dried in air [16]. The aqueous solution of pH 4.5 was prepared containing 0.02 M/0.1L $NiSO_4.7H_2O$, 0.02 M/0.1L Na_2MoO_4, 0.02 M/0.1L $ZnCl_2$ at room temperature (25 °C), for 30 minutes deposited on the stainless steel substrate which was used as a cathode at an applied voltage of -1.2 V relative to the reference electrode [11]. The potentiostatic curves for the Co-P_i (OEC) and NiMoZn-alloy (HEC) deposits are shown in Fig 2.

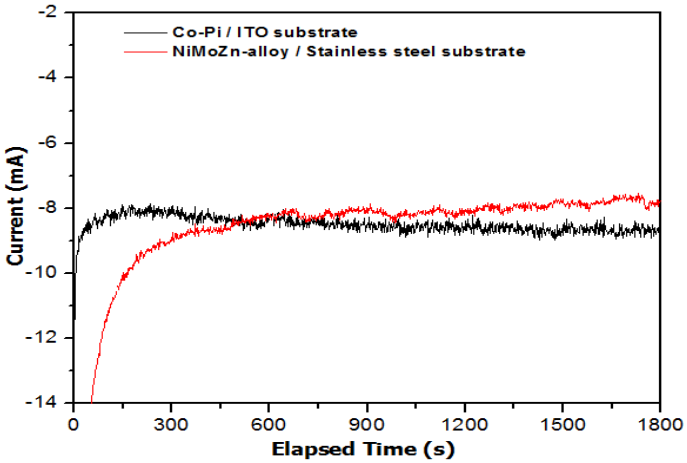

Fig. 2- Potentiostatic (I-t) curve for the Co-P_i (OEC) deposited over ITO coated electrode and NiMoZn-alloy (HEC) deposited over stainless steel electrode.

It is evident from the Fig 2 that by applying controlled voltage the current rapidly increases with respect to time and then it becomes nearly constant to a specific value. It is obvious from the figure that the elapsed time of 1800 seconds is enough time for metallic ions to migrate from the solution to the electrode where they will be deposited. The rate determining step of pulse electrodeposition is modulated by mass transport [18]. It is represented from the I-t curve that the respective current at the controlled potential of the working electrode for Co-P_i (OEC) was -8.670 mA and for NiMoZn-alloy (HEC) was -7.820 mA.

Further experiments were performed for increasing the hydrogen generation activity of the catalysts coated substrates when artificial leaf is put into the water. The thin films of Co-P_i (OEC) and NiMoZn-alloy (HEC) were deposited on bigger surface area substrates (7.5×7.5 cm^2) of ITO coated glass and stainless steel in order to increase the hydrogen generation activity of the catalysts coated substrates when artificial leaf is put into the water [19]. Direct current electrodeposition was performed for bigger surface area substrates by using the D.C. power supply. Both the substrates were used as cathodes during the electrodeposition. The electrodeposition was carried out only at one side of the cathode [16].

The direct current electrodeposition of Co-P_i (OEC) was performed using an ITO coated glass as cathode and graphite as anode of equal size (7.5×7.5 cm^2) and thus these electrodes were immersed in electrolyte of electrochemical cell. The aqueous solution of pH 7.0 was prepared containing 0.5 mM/0.3L $CoSO_4.H_2O$ and 0.1 M/0.3L K_2HPO_4. The prepared electrolyte was then deposited on ITO coated glass substrate which was used as a cathode, and kept at an applied voltage of 5.40 V at room temperature (25 °C) for 30 minutes [17]. The corresponding current at the controlled potential of the working electrode was recorded as 60 mA.

The direct current electrodeposition of NiMoZn-alloy (HEC) was performed by using stainless steel as cathode and graphite as anode of equal size (7.5×7.5 cm^2). The aqueous solution of pH 4.5 was used for electrodeposition of NiMoZn-alloy HEC containing 0.02 M/0.25L $NiSO_4.7H_2O$, 0.02 M/0.25L Na_2MoO_4, 0.02 M/0.25L $ZnCl_2$ at room temperature (25 °C), for 30 minutes deposited on the stainless steel substrate, and kept at an applied voltage of 3.85 V. The corresponding current at the controlled potential of the working electrode was 180 mA.

The D.C. electrodeposition of HEC was carried out without any additives but the catalytic activity for hydrogen generation was not very high when the catalysts coated solar cell was immersed in water. Therefore three additives were added in small amounts to enhance the catalytic activity for more hydrogen generation. Sodium pyrophosphate was used as a good complexing agent. Sodium bicarbonate was used as a supporting electrolyte to maintain pH during deposition. Hydrazine monohydrate was used as a reducing agent for the recovery of metals. The aqueous solution used for electrodeposition of NiMoZn-alloy HEC under additives contains 0.02 M/0.25L $NiSO_4.7H_2O$, 0.02 M/0.25L Na_2MoO_4, 0.02 M/0.25L $ZnCl_2$ with the addition of 0.5 mM/0.25L $Na_4P_2O_7.10H_2O$, 0.5 mM/0.25L $NaHCO_3$ and 0.1 mM/0.25L N_2H_4O.The prepared electrolyte was then deposited on stainless steel substrate at room temperature (25 °C) for 30 minutes, and kept at an applied voltage of 3.02 V. The respective current at the controlled potential of the working electrode was recorded as 20 mA.

The electrochemical aspects of the electrodeposition were investigated by cyclic voltammetry by means of Princeton Applied Research 263A potentiostat using the power suite software. Optical micrographs were captured by employing digital optical microscope (Olympus STM6). The surface morphology and elemental analysis of the electrodeposited films were examined with Scanning Electron Microscope (SEM) equipped with Energy Dispersive X-rays analysis (EDX) (Hitachi S-3000H).

3. RESULTS AND DISCUSSIONS

3.1. Electrochemical Analysis

The electrochemical behavior of the deposited films was established using cyclic voltammetry technique. Linear scan voltammetry is a convenient electrochemical method for analysis the phase structure of the deposits and also to detect the presence of metal on a surface [18]. The cyclic voltammetric curve (Fig. 3) for Co-P_i (OEC) and NiMoZn-alloy (HEC) deposits were obtained in the potential range between 0 and 1 V at a scan rate of 100 mVs^{-1} for 20 seconds.

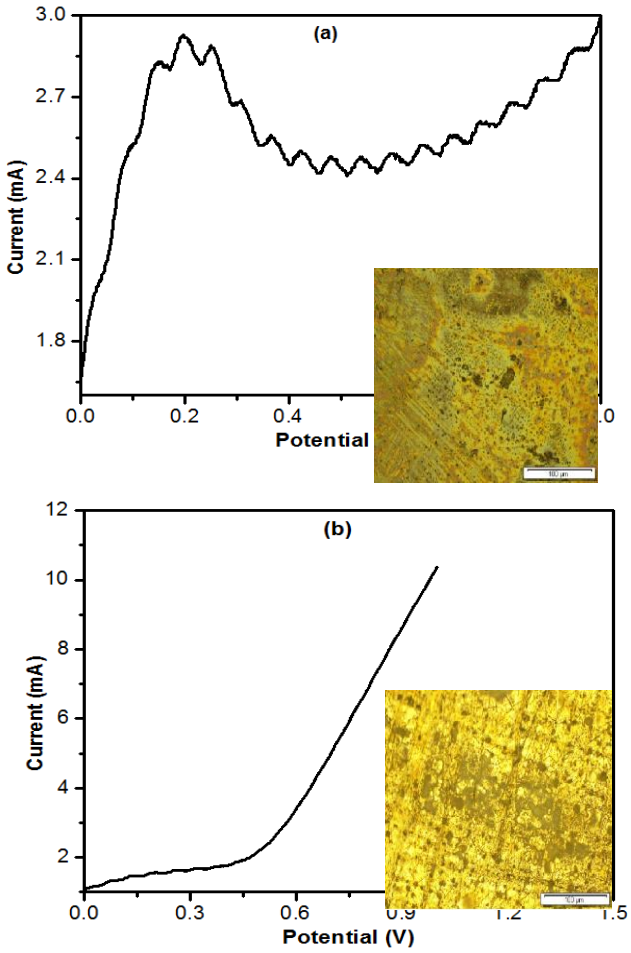

Fig. 3- Linear scan voltammetric curves of electrodeposited films at the scan rate 100 mV/s. (a) Co-P_i (OEC). (b) NiMoZn-alloy (HEC). Inset: Optical micrographs of the films deposited.

The cyclic voltammetric curve for Co-P_i (OEC) deposits, as shown in Fig. 3 (a), shows that the solid solution of cobalt sulfate and potassium hydrogen phosphate does not give separate peaks at their corresponding potential but continuous peaks that explicate the phase transition. The cyclic voltammetric curve for NiMoZn-alloy (HEC), as shown in Fig. 3 (b), represents the linear dependence of the current on the potential. The linear relation indicates that the process involved is the diffusion-control process [18]. The optical micrographs of the films confirmed the presence of the deposited material onto the surface of the substrate (inset of Fig. 3).

3.2. Surface morphology and elemental analysis

Surface morphology and elemental analysis of the Co-P_i and NiMoZn-alloy electrodeposited films at controlled voltages were investigated using Optical microscope, Scanning Electron Microscope (SEM) equipped with Energy Dispersive X-rays analysis (EDX).The micrographs and EDX spectra for the Co-P_i electrodeposited film are shown in Fig. 4.

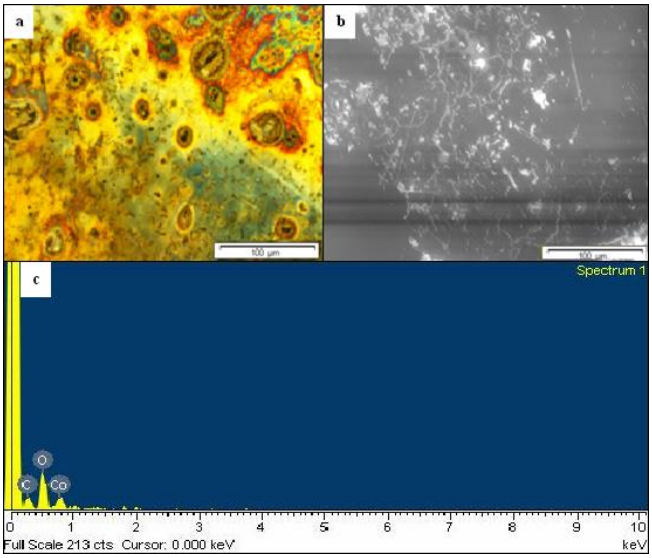

Fig. 4- The Co-P_i electrodeposited film. (a) Optical micrograph. (b) SEM micrograph. (c) EDX spectra.

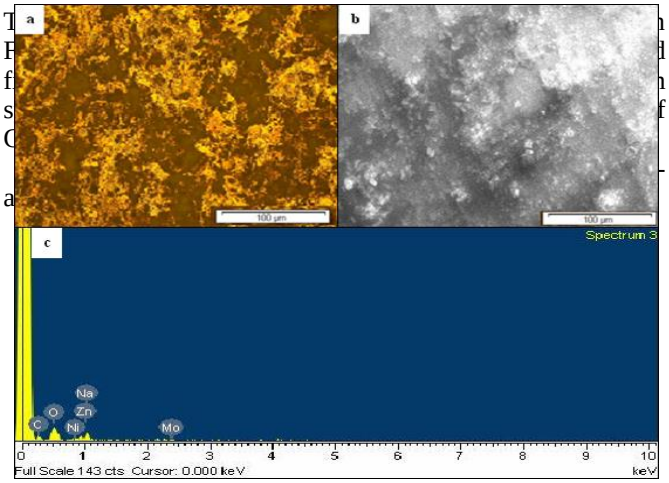

Fig. 5 - The NiMoZn-alloy electrodeposited film. (a) Optical micrograph. (b) SEM micrograph. (c) EDX spectra.

Fig. 5 (a) shows the optical micrograph of the film representing the non-uniform surface. Fig. 5 (b) shows the SEM micrograph of NiMoZn-alloy electrodeposited film. There are many micro-particles on the surface of the film as can see from the figure. Fig. 5 (c) shows that the EDX analysis of NiMoZn-alloy film synthesized by electrolyte of $NiSO_4.7H_2O$, Na_2MoO_4 and $ZnCl_2$ attests the presence of Ni, Mo, Zn, Na, O and C at the substrate surface.

The micrographs and EDX spectra for the NiMoZn-alloy electrodeposited film under certain additives are shown in Fig. 6.

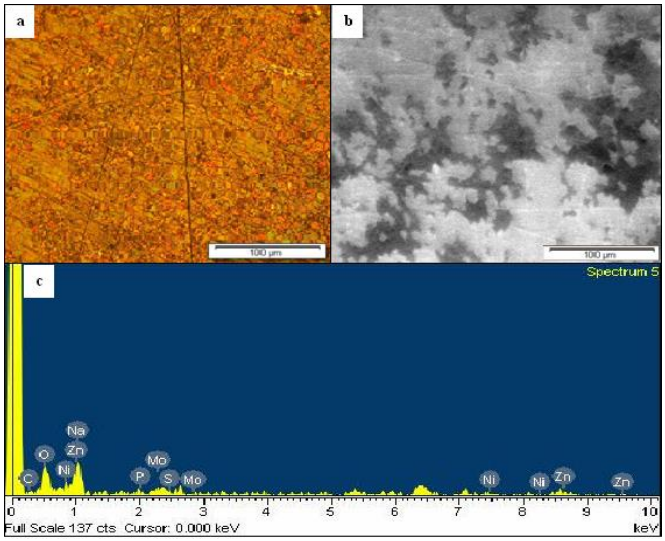

Fig. 6 - The NiMoZn-alloy electrodeposited film under additives. (a) Optical micrograph (b) SEM micrograph. (c)

EDX spectra.

Fig. 6 (a) shows the optical micrograph of the film representing the uniform surface. Fig. 6 (b) shows the SEM micrograph of NiMoZn-alloy electrodeposited film under additives representing the uniformity of the film. The growth of grains during electrodeposition is clearly evident and surface profile of the catalyst film is more uniform than Fig. 5 (b). Fig. 6 (c) shows the EDX analysis of NiMoZn-alloy film synthesized by electrolyte of $NiSO_4.7H_2O$, Na_2MoO_4 and $ZnCl_2$ under additives of $Na_4P_2O_7.10H_2O$, $NaHCO_3$ and N_2H_4O attests the presence of Ni, Mo, Zn, S, P, Na, O and C at the substrate surface.

3.3. H_2-generation Experiments

The H_2-generation experiment was performed using three artificial leaves. The small area leaf (1.5×1.5 cm^2) in which OEC and HEC were prepared by potentiostatic electrodeposition. The bigger area leaf (15×15 cm^2), in which OEC and HEC (without additives) were prepared by direct current electrodeposition. The bigger area leaf (15×15 cm^2), in which OEC and HEC (with additives) were prepared by direct current electrodeposition. Firstly H_2-generation was checked using artificial leaf A (1.5×1.5 cm^2) by placing it into the beaker filled with water and then exposed to sunlight from the n-side of the solar cell. The photographs in Fig. 7 show the generation of bubbles which manifests that the H_2-gas evolution from p-side of the solar cell (Fig.7a) and O_2-gas-evolution from the n-side of the solar cell (Fig.7b).

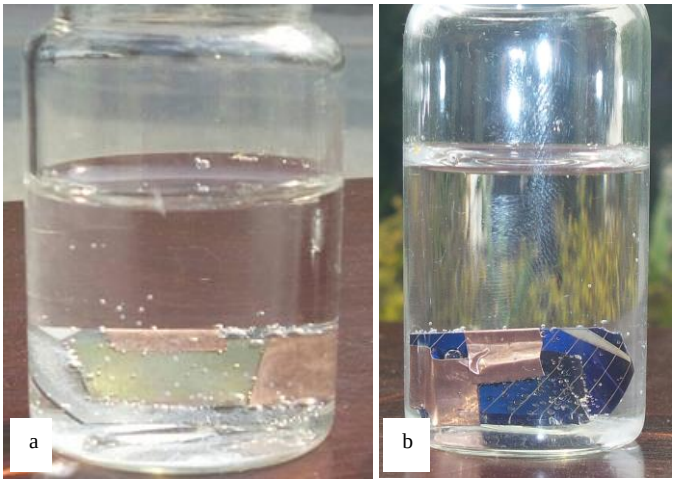

Fig. 7 - Bubbling experiment of artificial leaf A (a) H_2-Bubbles formation from the p-side of the solar cell. (b) O_2-Bubbles formation from the n-side of the solar cell.

It was observed from the figure that the average rate of H_2-evolution is 15 bubbles per cm^2 and for O_2-evolution is13 bubbles per cm^2 for artificial leaf A. The rate of bubbles generation for artificial leaf A is low.

Further H_2-generation experiment was performed for artificial leaf B (15×15 cm^2) having HEC without additives which was put into the beaker filled with water and then exposed to sunlight from the n-side of the solar cell. The generation of bubbles could be seen very straightforwardly: Hydrogen bubbles evolved from the p-side of the solar cell (Fig. 8a) and oxygen bubbles were evolving from the n-side of the solar cell (Fig. 8b). The photographs in Fig. 8 illustrate the bubbles generation activity of the artificial leaf B.

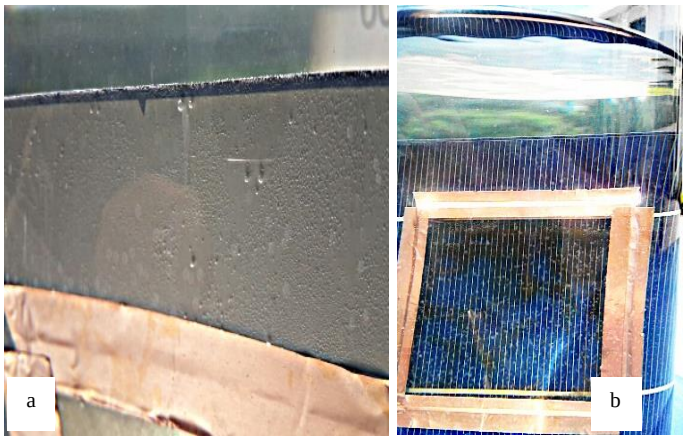

Fig. 8 - Bubbling experiment of artificial leaf B (a) H_2-Bubbles formation from the p-side of the Solar Cell. (b) O_2-Bubbles formation from the n-side of the Solar Cell.

It was observed from the figure that the average rate of H_2-evolution is 20 bubbles per cm^2 and for O_2-evolution is 18 bubbles per cm^2 for artificial leaf B. In the absence of additives, it was observed that the catalytic activity for the hydrogen generation is not very high. That's why we needed to add some additives to enhance the efficiency for hydrogen production. Third H_2-generation experiment was performed using artificial leaf C (15×15 cm^2) having HEC with additives which was put into the beaker filled water and then exposed to sunlight from the n-side of the solar cell. Enhanced generation of Hydrogen bubbles was observed from the p-side of the solar cell (Fig. 9a) and oxygen bubbles from the n-side of the solar cell (Fig. 9b). The photographs in Fig. 9 reveal clearly the enhanced generation of bubbles.

Fig. 9 - Bubbling experiment (a) Enhanced H_2-Bubbles formation from the p-side of the Solar Cell, (b) Enhanced O_2-Bubbles formation from the n-side of the Solar Cell.

It was observed from the figure that the average rate of H_2-evolution is 65 bubbles per cm^2 and for O_2-evolution is 50 bubbles per cm^2. In this experiment enhanced evolution rate was observed all over the surface of the artificial leaf C. The necessary data regarding for artificial leaf A, B and C is given in Table 1.

Table 1- Comparison of gas evolution rate per unit area in artificial leaf

Sample No.	H_2-generation experiment	Surface area of artificial leaf	No. of H_2-Bubbles per cm^2	No. of O_2-Bubbles per cm^2
Leaf A.	On small area deposited electrodes (1×1 cm^2)	1.5×1.5 cm^2	15	13
Leaf B.	On bigger area deposited electrodes (7.5×7.5 cm^2)	15×15 cm^2	20	18
Leaf C.	On bigger area deposited electrodes (7.5×7.5 cm^2) under additives	15×15 cm^2	65	50

4. CONCLUSIONS

The objective of this research work was to construct a wireless photocatalytic water splitting device for oxygen and hydrogen evolution on the large catalytic surface of the electrodes. The artificial leaf successfully accomplishes direct solar-to-fuel conversion by optimizing the performance of the electrodes using bigger area conductive electrodes. In the case of artificial leaf, the hydrogen is formed which can be stored directly or can be combined with CO_2 to make other

forms of energy such as carbon containing fuels. The construction of an efficient bigger area artificial leaf made possible by the OEC and HEC using additives for enhancing the water oxidation reaction and hydrogen evolution activity respectively. This water splitting device is required for practical solar-to-fuels systems. Artificial leaf provides an eminent approach to solve the energy challenges. This study opened the way to device an efficient water splitting catalytic system for clean fuel generation.

REFERENCES

[1] Amao Y, Hamano A, Shimizu K. Development of artificial leaf for solar hydrogen production. Energy Procedia 2013; 29: 21–25.

[2] Zhao Q, Yu z, Yuan W, Li J. Metal-C_i oxygen-evolving catalysts generated in situ in a mild H_2O/CO_2 environment. Int. J. Hydrogen Energy 2013; 38: 5251–8.

[3] Reece SY, Hamel JA, Sung K, Jarvi TD, Esswein AJ, Pijpers JJH, Nocera DG. Wireless Solar Water Splitting Using Silicon-Based Semiconductors and Earth-Abundant Catalysts. Sciencemag 2012; 334: 645–8.

[4] https://www.tamu.edu/faculty/bmiles/lectures/photosystems.

[5] Joya KS, Joya YF, Ocakoglu K, Krol RVD. Water-Splitting Catalysis and Solar Fuel Devices Artificial Leaves on the Move. Angew. Chem. Int. Ed. 2013; 52: 2–7.

[6] Arifin K, Majlan EH, Daud WRW, Kasim MB. Bimetallic complexes in artificial photosynthesis for hydrogen production: A review. Int. J. Hydrogen Energy 2012; 37: 3066–87.

[7] Elsegeiny M. Preliminary Experiments on Photo-Electro Catalytic Oxidation of Recalcitrant Organic Compounds Dissolved in Water. M.Sc. Thesis, University of New Orleans, Daytona Beach, 2013.

[8] Ager J. Fundamental Challenges in Solar to Fuel Conversion aka improving on Photosynthesis at JACP. Berkeley Lab. U.S. Department of Energy, Online Web 2/4/2014. http://www.nersc.gov/.

[9] Yang J, Wang D, Hongxian H, Li Can. Roles of Cocatalysts in Photocatalysis and Photoelectrocatalysis . Acc. Chem. Res. 2012; 1–10.

[10] Walter MG, warren EL, Mckone JR, Boettcher SW, Santori QMEA, Lewis NS. Solar Water splitting cells. Chem. Rev 2010; 110: 6446–73.

[11] Wang C, Li W, Lu X, Xie S, Xiao F, Liu P, Tong Y. Facile synthesis of porous 3D CoNiCu nano-network structure and their activity towards hydrogen evolution reaction. Int. J. Hydrogen Energy 2012; 37: 18688–93.

[12] Nocera D. The Artificial Leaf. Acc. Chem. Res. 2012; 45: 767– 76.

[13] Bachvarov VD, Arnaudova MH, Rashkov RRSt, Zielonka A. Electrochemical deposition of alloys based on Ni-Fe-Co, containing W, P, and their characterization for hydrogen evolution reaction. Bulg .Chem. Commun 2011; 43: 115–9.

[14] Lou HH, Huang Y. Electroplating. Encyclopedia of Chemical Processing. 2006; 1-10.

[15] Subramania A, Priyaa ARS, Muralidharan VS. Electrocatalytic Behavior of Nickel-Cerium Alloy Deposits. Port. Electrochim. Acta 2007; 25: 481–88.

[16] Rahman MJ, Sen SR, Moniruzzaman M, Shorowordi KM. Morphology and properties of Electrodeposited Zn-Ni Alloy coatings on mild steel. J .Mech. Eng. Res 2009; 40: 1–6.

[17] Surendranath Y, Dinca M, Nocera DG. Electrolyte-Dependent Electrosynthesis and Activity of Cobalt-Based Water Oxidation Catalysts. J. Am. Chem. soc. 2009; 131: 2615–20.

[18] Foyet A. Electrochemical deposition of Cobalt, Nickel-Cobalt, Nickel-Copper and Zinc-Nickel nanostructured materials on aluminum by template self- organization. Institute of natural sciences, M.Sc. thesis. Physics and chemistry Martin Luther University Halley-Wittenberg, Germany, 2007.

[19] Krishnan P, Advani SG, Prasad AK. Cobalt oxides as Co_2B catalyst precursors for the hydrolysis of sodium borohydride solutions to generate hydrogen for PEM fuel cells. Int. J. Hydrogen Energy 2008; 33: 7095–102.